

1 **Iterative species distribution modeling results in the discovery of novel**
2 **populations of a rare cold desert perennial**

3
4 **Running title: Iterative species distribution modeling**

5
6 Israel T. Borokini^{1,2,*}, Kenneth Nussear³, Blaise Petitpierre⁴, Thomas E. Dilts⁵, Peter J. Weisberg⁵

7 ¹Ecology, Evolution and Conservation Biology graduate program, Department of Biology,
8 University of Nevada, Reno, Reno NV 89557

9 ²Department of Integrative Biology, University of California, Berkeley, Berkeley CA 94720

10 ³Department of Geography, University of Nevada, Reno, Reno NV 89557

11 ⁴Institute of Earth Surface Dynamics, University of Lausanne, Lausanne CH-1015, Switzerland

12 ⁵Department of Natural Resources and Environmental Science, University of Nevada, Reno,
13 Reno NV 89557

14 *Corresponding author: iborokini@berkeley.edu; ORCID: 0000-0002-1258-7932

15 **ABSTRACT**

16 Niche modeling for rare and range-restricted species can generate inaccurate predictions
17 leading to an overestimation of a species geographic distribution. We used an iterative
18 ensemble modeling approach and model-stratified field surveys to improve niche model
19 formulation and better understand the ecological drivers of *Ivesia webberi* distribution. *I.*
20 *webberi* is a U.S. federally threatened herbaceous species, narrowly distributed in the Western
21 Great Basin Desert. Niche models for *I. webberi* were fitted using 10 replicates each of six
22 modeling algorithms, while geographical projections of habitat suitability were generated
23 using weighted ensembles of models with optimal performance. The resulting model
24 projections were used to guide field surveys for five years, generating additional spatial data,
25 which were added to the existing dataset for subsequent modeling. Model performance across
26 iterations was investigated, while niche differences in the spatial dataset were explored.
27 Model-guided field surveys resulted in the discovery of several new locations of *I. webberi* and
28 an expansion of the species' known range by 63 km. Model performance was higher in the
29 earlier but overfitted niche models; overfitting was corrected in the final models, while
30 predicted habitat suitability was reduced by 50%. Findings show that *I. webberi* niche is
31 associated with biotic, topographic and bioclimatic variables. Further, a partial overlap was
32 observed between environmental conditions of the initial and new locations (Schoener's
33 $D=0.47$), which can be decomposed into 93% of niche stability. This indicates that the majority
34 of the newly discovered locations are within the environmental niche of the initial data.

35 **KEYWORDS:** habitat suitability, iterative ensemble modeling, niche overlap, field validation
36 surveys, niche stability, *Ivesia webberi*, Great Basin Desert

37 1. INTRODUCTION

38 Limited empirical information on the geographical distributions of taxa (Wallacean
39 shortfall; Whittaker et al. 2005) can impact the assessment of species rarity resulting in
40 misguided conservation prioritizations (Coddington et al. 2009). Field surveys, especially those
41 conducted using random sampling strategies, can generate additional biodiversity data to
42 mitigate this; however, such surveys are costly, time-consuming, and ineffective for rare
43 species, while human resources are limited (Hirzel & Guisan 2002, Guisan et al. 2006).
44 Therefore, scientists and conservation managers have considered other cost-effective methods
45 to stratify and prioritize field surveys, using, for example, expert opinion and quantitative
46 niche modeling. Niche models can relate species' occurrences to their environmental
47 conditions to quantify the realized niche, that is, species' known locations due to
48 environmental tolerance observed in the field (Hutchinson 1957). These niche models generate
49 geographic predictions of species habitat suitability that can be used to stratify and optimize
50 sampling efficiency (Chiffard et al. 2020). Moreover, integrating the new spatial data from
51 model-guided sampling can reduce spatial bias in subsequent modeling iterations, improve
52 the predictive accuracy of niche models for rare species, and reliably identify biologically-
53 relevant environmental factors (Singh et al. 2009, Rinnhofer et al. 2012).

54 Understanding the distribution of rare species is critical for effective conservation
55 planning, but with few, incomplete, and biased spatial data, it can be challenging to model the
56 niches of rare species with high predictive accuracy (Hernandez et al. 2006, Wisz et al. 2008), a
57 condition referred to as the rare species modeling paradox (Lomba et al. 2010). This is because
58 fewer occurrence points in spatial dataset indicates low prevalence, which weakens the

59 analytical power of the models and inflates bias in niche models (Vaughan & Ormerod 2003).
60 Furthermore, correlative species distribution models include the underlying assumption that
61 species are in equilibrium with their environment (i.e., temporal and spatial stationarity), and
62 that all important and biologically-relevant variables have been included in the niche model
63 (Elith & Leathwick 2009). This presents challenges to modeling rare species because the
64 inclusion of many predictors when occurrences are few can lead to model overfitting (Wisz et
65 al. 2008, Jarnevich et al. 2015). Moreover, limited natural history knowledge makes predictor
66 variable selection challenging and potentially subjective for rare species (Aranda & Lobo 2011).
67 Consequently, poorly fit models and misjudgments of model predictions can lead to over- or
68 underestimation of the species' niche, resulting in poorly informed management decisions
69 (Ramesh et al. 2017, Burns et al. 2020). Despite the development of several statistical methods
70 to reduce prediction errors in niche modeling, the most practical way is to increase spatial data
71 for rare species, which is inevitably linked with data collection during field surveys. Therefore,
72 predictions of species distribution modeling (SDM) for rare species should not be treated as
73 truth, but can be used as hypotheses for further ecological or biogeographical investigations
74 (Stockwell & Peterson 2002, Jarnevich et al. 2015, Sofaer et al. 2019).

75 The discovery of new locations of targeted species from SDM-guided field surveys is
76 well documented in the literature (e.g., Williams et al. 2009, de Siqueira et al. 2009, Särkinen et
77 al. 2013, Burns et al. 2020). These novel discoveries underscore the importance of SDMs as an
78 important conservation tool. SDMs have been used to evaluate the degree of species rarity
79 (Broennimann et al. 2006), and identify areas that may serve as future climatic refugia (Sousa-
80 Silva et al. 2014). Furthermore, SDMs are also used to advance scientific knowledge of species-

81 environment relationships (Jiménez-Valverde et al. 2011), and identify niche constraining
82 environmental factors (Gorban et al. 2011). SDM predictions are often integrated into models
83 of population and landscape genetics (e.g., Ikeda et al. 2016, Banerjee et al. 2019), and spatial
84 phylogenetics (e.g., Thornhill et al. 2017). Beyond conservation uses, newly discovered
85 occurrences may have significant ecological contributions to the understanding of the overall
86 species' niche. For example, additional occurrence points may be found either within the
87 existing realized niche space or in areas with different ecological conditions, thus expanding
88 the species environmental niche. The COUE (that is, centroid shift, overlap, unfilling, and
89 expansion) framework can be used to quantify realized niches of species from different ranges
90 and categorize the niche position of newly discovered occurrences (Broennimann et al. 2012).
91 This framework has been used to investigate niche dynamics between the native and invaded
92 ranges of invasive species (Broennimann et al. 2012, Strubbe et al. 2013), as well as niche
93 evolution vs conservatism between sister taxa (Villegas et al. 2021).

94 The aim of this study was to assess relative improvement of using iterative sampling
95 approach alternating between niche modeling and model-guided field surveys relative to a
96 presence/absence modeling approach using only data available at the onset of the study to
97 predict the distribution of a rare plant (*Ivesia webberi* A. Gray). Therefore, we asked the
98 following questions: (1) Which environmental variables determine the distribution of *I.*
99 *webberi*, and how does the species-environment relationship change with each iteration of the
100 SDMs given additional spatial data? (2) Do additional distribution data alter habitat suitability
101 map projections across modeling iterations? (3) Is the environmental niche conserved

102 throughout the modeling iterations? (4) Do modeling iterations improve the predictive
103 accuracy of species distribution models for *Ivesia webberi*?

104

105 **2. MATERIALS AND METHODS**

106 **2.1. Study species and study area**

107 *Ivesia webberi* is a U.S. federally listed threatened perennial forb restricted to the eastern
108 foothills of the Sierra Nevada and the adjacent western edge of the Great Basin Desert. *I.*
109 *webberi* was estimated to have originated between 1.3 and 3.8 million years ago (Töpel et al.
110 2012), and may be one of the many Great Basin Desert neoendemic and phylogenetically
111 young taxa that have not had enough time to fully colonize their range (Kraft et al. 2010,
112 Thornhill et al. 2017). At the outset of our study, it was known from 23 spatially-aggregated
113 locations, occurring in or near ephemeral washes and dry forest meadow gaps in mostly
114 gently sloped areas (Witham 2000). These presence locations were visited multiple times
115 between 2015 and 2020, and therefore are not prone to positional error. These locations have
116 experienced varying degrees of biological invasion pressures from *Bromus tectorum*,
117 *Taeniatherum caput-medusae*, and *Poa bulbosa*, as well as disturbances from wildfires, cattle
118 grazing and off-highway vehicle use.

119 The study extent was defined by a 60 km buffer from marginal ranges of known
120 populations as of 2015. The species produces achenes which are not adapted for long-range
121 dispersal; therefore, the study area was restricted to mask out expansive adjacent unsuitable
122 areas of playas in the central Great Basin Desert. This modeling decision was guided by
123 natural history indicating that the species is located in sparsely vegetated low sagebrush

124 (*Artemisia arbuscula*) communities in mid-elevation areas of the western Great Basin Desert and
125 the adjacent northern Sierra Nevada eastern foothills (US Fish and Wildlife Service [USFWS]
126 2014). Climatic conditions in these sites are characterized by relatively mild winters and hot
127 summers (Svejcar et al. 2017). Thus, temperatures range from an average of -5.8 °C in the
128 winter to an average of 28 °C in the summer, while annual precipitation varies between 25 and
129 33 cm, most of which falls as snow or rain during the winter months.

130 **2.2. Distribution data**

131 We began species distribution modeling in 2015 with 23 occurrence points and 758
132 absence points obtained from the Nevada Natural Heritage Program (NNHP). The absence
133 points represent areas where *I. webberi* was not detected during historical surveys by NNHP
134 botanists and citizen scientists. Additional spatial points were added following iterative
135 modeling and field validation cycles in predicted suitable habitats. In all modeling iterations,
136 the absence points were thinned using a distance of 7.5 km in *spThin* R package version 0.2.0
137 (Aiello-Lammens et al. 2015) to reduce the effects of spatial aggregation, and mitigate low
138 prevalence in the spatial dataset. Additionally, absence points within 5 km of an occurrence
139 point were removed to avoid false negatives. The remaining absence points were merged with
140 the presence points for niche modeling (Table 1).

141 **2.3. Predictor variables**

142 A total of 72 predictor variables describing edaphic, topographic, land cover, vegetative
143 cover, and climatic factors were assembled for fitting SDMs for *Ivesia webberi* (see Table S1). To
144 avoid overfitting and maintain a 1:10 ratio of predictor variables to occurrence points (Harrell
145 et al. 1996), the full set of predictor variables was reduced to six uncorrelated predictors (Table

146 2) using a combination of the Kendall r correlation coefficient ($r > 0.6$), feature selection runs in
147 *Boruta* R package version 4.0.0 (Kursa & Rudnicki 2010), and recursive feature elimination
148 algorithm in *caret* R package version 6.0-78 (Kuhn 2008).

149 The climatic variables (actual evapotranspiration, minimum monthly temperature and
150 summer seasonal precipitation) were downsampled from the Parameter-elevation
151 Relationships on Independent Slopes Model (PRISM) climatic data (1971-2000) normals (Daly
152 et al. 2008), from 800-m to 30-m spatial resolution using the Climatic Water Deficit Toolbox
153 (Dilts et al. 2015) and ordinary kriging. The cosine-transformed aspect, ranging from -1 (south-
154 facing slope) to +1 (north-facing slope), was derived from slope using the formula: $\theta \times \cos(\alpha)$,
155 where θ is slope (in percentage), and α is aspect (in radians), while slope was calculated from
156 the 1 arc-second digital elevation models (DEM; United States Geological Survey [USGS]
157 2017). Perennial herbaceous vegetative cover, a vegetation type raster layer, was obtained from
158 the Multi-Resolution Land Characteristics (MRLC) development of the 2016 U.S. National
159 Land Cover Database (NLCD; Xian et al. 2013). Topographic Position Index (TPI) was
160 calculated from the DEM using the formula described by Weiss (2001).

161 **2.4. Iterative ensemble niche modeling and model-based sampling**

162 The SDMs were fitted at 30 m resolution to capture the landscape and ecological
163 heterogeneity in the study area, particularly in the *Ivesia webberi* locations that occur within
164 forest gaps. An ensemble modeling approach was used in all niche modeling iterations. The
165 use of multi-algorithm ensemble models renders predictions less susceptible to biases,
166 assumptions, or limitations of any individual algorithm, while broadening the types of
167 environmental response functions that can be identified (Araújo & New 2006). SDMs have

168 been developed from a wide range of modeling techniques including regression, classification,
169 and machine learning algorithms (Lauzeral et al. 2012). Because these algorithms have
170 different predictive performances under different contingencies (Li et al. 2013), fitting of niche
171 models using different algorithms and combining their model parameters to build a consensus
172 or ensemble model is often recommended (Marmion et al. 2009). Ten replicates of six
173 algorithms (Boosted Regression Trees, Random Forests, Maximum Entropy, Artificial Neural
174 Networks, Generalized Additive Models and Generalized Linear Models) were fitted using the
175 *biomod2* R package (Thuiller et al. 2009). All statistical packages were implemented in R
176 statistical software version 4.0.2 (R Core Team 2020). See Table S2 for modeling details.

177 Model performance was evaluated using four metrics, including true skill statistic (TSS;
178 Allouche et al. 2006), area under the curve (AUC) of the receiver operating characteristics
179 (ROC) plot (Hanley & McNeil 1982), TSS-based specificity, and Boyce Index (Boyce et al. 2002).
180 In each modeling iteration, three predictors, selected from the six uncorrelated variables, were
181 used to fit the niche models. Models were fitted with 80% of the data with 20% used for k-fold
182 cross-validation (Araújo et al. 2005, Thuiller et al. 2009). Model replicates with $TSS \geq 0.7$ were
183 averaged into ensemble models, which were used to produce geographic projections of habitat
184 suitability (Marmion et al. 2009, Thuiller et al. 2009). On the habitat suitability maps, cells with
185 ≥ 0.5 occurrence probability were considered suitable to delineate areas with higher habitat
186 suitability values for field validation surveys. Uncertainty in habitat suitability projections was
187 visualized on maps of coefficients of variation from the iterative niche ensemble models
188 (Hortal 2008).

189 Habitat suitability maps produced by the SDMs were used to guide field validation
190 surveys to areas of high predicted probability of occurrence. The non-thinned absence points
191 were overlaid on the predicted habitat map and predicted suitable and unsuitable areas that
192 had not been previously surveyed were selected for field validation. Field validation surveys
193 were done alone by the first author (I.T.B.), between May and June of each year when the
194 plants were in flower, to increase chances of detection. Additional spatial data from field
195 surveys were used in the subsequent modeling iteration and site selection for post-modeling
196 field validation. The iterative modeling and field surveys were repeated for five years. For
197 each newly discovered population, we calculated the distance to the nearest previously known
198 occurrence with the *FNN* R package version 1.1.3 (Beygelzimer et al. 2019).

199 The relative importance of the predictor variables in all iterative SDMs was evaluated
200 using the jackknife test (Phillips et al. 2006), while species-environment relationships were
201 described with partial response curves using the evaluation strip method (Elith et al. 2005) as
202 implemented in the *biomod2* R package. We assessed the trends and statistical significance of
203 the model performance across the years of iterative niche modeling, to investigate if additional
204 spatial data improved the overall predictive accuracy of the iterative ensemble SDMs. Mean
205 scores of the four model performance metrics for each of the six algorithms (10 replicates each)
206 were regressed against the years of iterative SDMs using multivariate multiple linear
207 regression (MMLR), while the statistical significance of the MMLR models were corrected
208 using the Tukey post-hoc test.

209 We also assessed the reliability of these iterative SDM predictions by checking for
210 model overfitting with a spatial cross-validation approach using block partitioning. Spatial

211 block partitioning is a nonrandom allocation of spatial data to reduce the effect of spatial bias
212 and autocorrelation in ecological models (Valavi et al. 2019). The entire study area was divided
213 into six equal latitudinal and longitudinal bins, which were then clustered into three spatial
214 blocks. Two spatial blocks were used for model training while the third block was used for
215 testing. Spatial block partitioning was done in the *blockCV* R package version 2.1.4 (Valavi et al.
216 2019), while the niche models were conducted in *biomod2* R package version 3.5.1, using
217 similar model tuning as used for the iterative SDMs. Partitioning our relatively small spatial
218 dataset could only meet the requirements for modeling with random forest, maximum
219 entropy, and artificial neural networks, which were used for the spatial block-based ensemble
220 niche modeling. Overfitting was assessed as the difference between the block (training) and
221 test AUC values (Warren & Siefert 2011).

222 **2.5. Assessment of the change in *I. webberi* niche across modeling iterations**

223 We used the COUE framework to investigate the position of the new locations relative
224 to the initial niche of *I. webberi*. The COUE framework, based on the principal component
225 analysis (PCA), allows for direct comparison of species-environment relationships
226 (Broennimann et al. 2012). A kernel density function is applied to smooth the varying
227 sampling sizes in the two sets of occurrence points in a PCA gridded environmental space to
228 calculate the niche metrics (Petitpierre et al. 2012, Broennimann et al. 2012). We calculated
229 niche overlap (Schoener's *D*), stability, expansion, and unfilling between the initial (2015) and
230 a combination of all new (2018-2020) *I. webberi* locations, based on the environmental space of
231 the six uncorrelated predictor variables. Schoener's *D* is calculated between the environmental
232 occupancy of the two niches, and it ranges between 0 (no overlap) and 1 (total overlap) which

233 represent niche divergence and similarity, respectively (Brown & Carnaval 2019). In this study,
234 niche stability represents the proportion of the environmental space in the newly discovered
235 locations available in the initial occurrences' environmental space, while niche expansion
236 represents the proportion of the environmental space in the new locations that are not
237 available in the initial locations. A niche unfilling estimate was used to investigate whether the
238 new occurrences only colonized a limited portion of the environmental space of the initial
239 occurrences (Petitpierre et al. 2012, Guisan et al. 2014). The COUE framework was
240 implemented using a niche similarity test, which assumes that the environmental niches in the
241 new occurrences are similar to the initial occurrences, given that habitat suitability map
242 projections of the initial occurrences were used for field validation surveys (Liu et al. 2020, Pili
243 et al. 2020). The niche similarity test generated random estimates for each of Schoener's D ,
244 niche stability, expansion and unfilling, using 1000 randomizations of the niche positions of
245 the initial and newly discovered occurrences. These randomizations were used to check if the
246 observed niche overlap and stability were higher and if observed niche expansion and
247 unfilling were lower than expected by chance. Furthermore, we extracted values of the initial
248 niche density at the new locations to quantify the degree of niche stability or expansion in the
249 new locations. Niche density values range from 0 to 1; 0 represents new locations outside the
250 initial niche (that is, niche expansion), while 1 represents new locations in the core of the initial
251 niche. The niche similarity test was run with the development version 3.2.1 of the *ecospat* R
252 package available on *github* (Broennimann et al. 2016).

253 Additionally, we quantified the number of predicted suitable raster cells (≥ 0.5
254 probability of occurrence) in the habitat suitability maps. We also performed a niche overlap

255 analysis on the geographic projections of habitat suitability between the 2015 (initial) and 2020
256 (final) model iterations for each iterative niche model, using the *I* similarity metric, which is
257 based on Hellinger distance (Warren et al. 2008). The *I* similarity metric ranges from 0 to 1
258 representing the degree of pairwise similarity in niche model projections (Warren et al. 2008).
259 This map-based niche overlap test is a cell-by-cell comparison with a randomization test of
260 geographical predictions of the four iterative SDMs (Warren et al. 2008); it was performed in
261 the *dismo* R package (Hijmans et al. 2017).

262

263 3. RESULTS

264 3.1. Which environmental variables are associated with the ecological niche of *I. webberi*, 265 and how does our understanding of these species-environment relationships change across 266 the SDMs?

267 Throughout the iterative SDMs from 2015 to 2020, the perennial herbaceous vegetative
268 cover consistently contributed the most to the fitted distribution of *I. webberi* (Fig. 1a-d). In the
269 2020 model iteration, *I. webberi* showed an asymmetric and threshold response curve for
270 perennial vegetative cover, with suitable sites occurring in areas with moderate (>20%) to high
271 native perennial forb cover (Fig. 2a). Topographic Position Index (TPI) was the second most
272 important predictor across all model iterations. The response curve for TPI is bimodal and
273 asymmetric, illustrating that *I. webberi* occurs on sites that are either gentle lateral valleys or
274 ridges (Fig. 2c). AET was the third most important predictor in the 2015 niche model iteration
275 (Fig. 1a). The cosine-transformed slope aspect, a proxy for exposure to sunlight, came third in
276 the 2018 and 2019 iterations (Fig. 1 c and d), while summer seasonal precipitation was the third

277 most important predictor for the 2020 iteration (Fig. 1d). The response curve for summer
278 seasonal precipitation shows a threshold response, where the probability of *I. webberi*
279 occurrence was maximized at >25 mm summer precipitation, beyond which the curve
280 flattened (Fig. 2b).

281 **3.2. Does the additional spatial data impact *I. webberi* niche dynamics and habitat** 282 **suitability map projections across modeling iterations?**

283 The iterative ensemble SDMs and model-guided field surveys resulted in the discovery
284 of seven new locations of *I. webberi* (30.4% of the initial dataset), while two additional new
285 locations (8.7% of the initial dataset) were discovered opportunistically by local botanists. The
286 distance from the new locations to the closest known locations ranged from 30 m to 63 km
287 (Table 3). As a result, the northern distribution range of the species was expanded by 63 km
288 (Table 3). However, the percentage of the suitable raster cells in the ensemble habitat
289 projections decreased from 5.98% in 2015 to 3.34% in 2020 (Fig. 3 a-d). Despite the decrease in
290 the percentage of suitable grid cells, niche overlap between the geographical projections of the
291 2015 and 2020 model iterations were high (Hellinger's $I=0.89$). The model projections also
292 predicted higher probability of *I. webberi* occurrence in locations near the center of the study
293 area (Fig. 3 a-d). Prediction uncertainties (coefficients of variation) were relatively low across
294 all four projections (Fig. 4 a-d).

295 **3.3. Is *I. webberi* environmental niche conserved throughout the modeling iterations?**

296 The first two PCA axes explained 49% of the variation in the data, both of which
297 represent topo-climatic gradients (Figure 5, Table S3), while the third axis, representing the

298 perennial vegetation cover, explained an additional 17.4% of the variance (Table S3). The PCA
299 niche similarity test shows that the environmental niche of the new occurrences overlaps that
300 of the initial occurrences with marginal significance (Schoener's $D=0.47$; $p=0.05$). This finding
301 was corroborated by the niche stability result showing that the environmental niche of the new
302 occurrences is similar to the initial occurrences (niche stability=0.93; Fig. 5), although this high
303 value was marginally significant ($p=0.09$; Fig. 6). Furthermore, the values of the new locations
304 in the niche density of the initial occurrences ranged from 0.21 to 0.87 (Table 3), which shows
305 that all of these new points are found within the initial niche, thus, niche stability. However,
306 niche changes between the initial and new occurrences are due to unfilling (estimate=0.47;
307 $p=0.11$) rather than expansion (estimate=0.07; $p=0.09$; Fig. 6). The majority of the randomized
308 niche overlap and stability estimates were lower than the observed values (Fig. 6a & b,
309 respectively), while the majority of the randomized expansion and unfilling estimates were
310 higher than the observed values (Fig. 6c & d, respectively).

311 **3.4. Do modeling iterations improve the predictive accuracy and reliability of the SDMs for** 312 ***Ivesia webberi*?**

313 Figures 7a-d shows the mean performance metrics for the iterative ensemble SDMs
314 between 2015 and 2020. The TSS-based model performance scores significantly decreased from
315 0.81 in 2015 to 0.78 in the 2020 model iterations (Tukey post-hoc: $p=0.01$). Similarly, the AUC
316 scores significantly decreased from 0.89 to 0.82 between the 2015 and 2020 model iterations
317 respectively (Tukey post-hoc: $p=0.02$). However, both Boyce Index and specificity showed
318 nonsignificant ($p>0.05$) changes between 2015 and 2020 model iterations (0.44 to 0.41, and 92.04
319 to 95.58, respectively). The predictive performance of the spatial block niche modeling for the

320 2015 spatial data indicates model overfitting ($AUC_{BLOCK}=0.81$, $AUC_{TEST}=0.47$), in contrast to
321 the 2020 spatial data which did not exhibit overfitting ($AUC_{BLOCK}=0.47$, $AUC_{TEST}=0.52$).

322

323 4. DISCUSSION

324 Within a five-year period, our iterative modeling approach resulted in the discovery of
325 nine novel locations (representing 39% of the initial known distribution) and a 63 km
326 expansion of the predicted geographical range of a federally threatened perennial forb. The
327 discovery of new locations from model-guided field surveys is frequently reported for rare
328 species in the literature, and highlight the importance of SDMs and model-guided field
329 surveys in conservation. As a result of enlarged occurrence datasets and known ranges, many
330 threatened species have subsequently been delisted from the Endangered Species Act (Keinath
331 et al. 2014, Sofaer et al. 2019). Moreover, with sufficient spatial data, models can reliably
332 identify biologically relevant ecological factors that support species persistence and predict
333 their potential distributions. In this study, the number of *I. webberi* occurrences increased by
334 39% (from $n=23$ to $n=32$) and *I. webberi* patch occupancy in many of the new locations
335 compares well with those of the original locations. Therefore, findings from this study can
336 guide decisions on future *I. webberi* management. Moreover, previous studies have also
337 reported major revisions to conservation management and reserve designs due to the
338 additional biodiversity data from model-guided field surveys (Platts et al. 2010), including
339 decisions regarding translocation of species of conservation concern (Draper et al. 2019).
340 Findings of multiple analyses show that the majority of the new locations are found within the
341 environmental niche of the initial occurrences. We observed high niche stability (93%) and low

342 niche expansion (7%) between the environmental conditions in the initial and new
343 occurrences, while both the initial niche density values of the new locations and the niche
344 dynamics plot (Fig. 5) illustrate the position of the new locations within the realized niche
345 space of the initial occurrences. This is not surprising considering that the field validation
346 surveys that resulted in the discovery of these novel locations were based on initial models.
347 The observed niche overlap and stability estimates are higher than the majority of the
348 randomly generated niches, whereas niche unfilling and expansion are lower than most of the
349 random niches generated in the similarity test (Fig. 6). In spite of the nonsignificant
350 randomization results, these findings provide partial support for niche similarity between the
351 initial and novel occurrences. The marginally significant randomizations ($0.05 < p < 0.15$) could
352 be attributed to a limited statistical power due to the low number of occurrences and high
353 degree of geographical similarity in both the initial and new datasets (Brown & Carnaval
354 2019). The unfilled portion of the niche (Fig. 5) suggests that there may be more *I. webberi*
355 locations yet to be discovered or suitable habitat yet to be colonized due to the species' limited
356 dispersal capacity.

357 Additional spatial data can significantly impact the predictive performance of iterative
358 niche models, due to their effect on model parameters (Guisan et al. 2006). In this study, we
359 observed changes in model performance and geographical projections, despite the minimal
360 changes in the three predictors used across all model iterations. Specificity is based on
361 omission error rates, which represent the percentage of false negatives in the spatial data.
362 Therefore, slight increases in specificity across the model iterations suggest that the additional
363 spatial data slightly reduced presence-absence ratio in the overall spatial data and also

364 reduced the model omission errors (Lauzeral et al. 2012, Chiffard et al. 2020). However, the
365 reduction of AUC, TSS, and Boyce Index in all but the final model iteration may be attributed
366 to overfitting due to insufficient occurrences in the dataset. Additional spatial datasets from
367 multi-year sampling may have corrected model overfitting, but they also resulted in reduced
368 SDM performance. This is consistent with previous studies that also reported reduced niche
369 performance when correcting overfitting in niche models (Guisan et al. 2006, Peterson et al.
370 2007). Therefore, a fair performance assessment for iterative niche modeling should focus on
371 model generalizability as the primary measure of performance as opposed to model fit for any
372 given year. A rigorous approach to assessing model generalizability (or lack of over-fitting) is
373 to use spatially independent data for model validation, as in the spatial block niche modeling
374 approach employed in this study. Secondly, some of the additional absence points were
375 sampled from areas that were predicted to be suitable. This can introduce noise into spatial
376 data used for iterative niche modeling because the absence of *I. webberi* in these predicted
377 suitable sites may be due to dispersal limitation (Lobo et al. 2010, Lauzeral et al. 2012). Field
378 observations support the suitability of some of these surveyed sites because they have similar
379 edaphic and topographic features and the occurrence of common associates like *Balsamorhiza*
380 *hookeri*, *Artemisia arbuscula*, *Antennaria dimorpha*, and *Phlox longifolia*. McCune (2016) reported
381 similar circumstances where common floristic associates of several studied plants were found
382 in sites predicted to be suitable. Therefore, the inclusion of such absence points in iterative
383 niche models can result in the underprediction of the potential niche and a reduction in model
384 performance (Araújo & Peterson 2012).

385 The biology of a species may also affect the predictive performance of niche models
386 (Marmion et al. 2009, Regos et al. 2019), and particularly the performance of iterative SDMs
387 following the addition of new spatial data (Guisan et al. 2006, Lauzeral et al. 2012). Despite its
388 relatively restricted geographical range, *I. webberi* is locally abundant in occurrence locations
389 and it exhibits mixed mating system (Borokini et al. 2021). These traits suggest high
390 colonization potential and wider niche breadth (Grant & Kalisz 2019), which fits the
391 description of satellite-type species (Hanski 1982, Collins et al. 1993). For satellite-type species,
392 low dispersal capacity limits the full colonization of suitable habitat and may reduce
393 predictive performance of SDMs (Edwards et al. 2004). Araújo & Peterson (2012) cautioned
394 that areas of commission errors should be interpreted carefully for species with fewer
395 occurrences because they may represent suitable habitats that are yet to be colonized (that is,
396 potential niche). This may be true for the neo-endemic *I. webberi* which may not yet be in
397 equilibrium with its suitable environment (Araújo & Pearson 2005) because it has not yet fully
398 colonized its range (Kraft et al. 2010, Thornhill et al. 2017). To reduce spatial bias in iterative
399 SDMs, additional spatial data must be collected using stratified sampling from both sites with
400 predicted higher and low probabilities of species occurrence (Edwards et al. 2004, Guisan et al.
401 2006). Additionally, absence points too close to presence points in ordination space (thus
402 sharing similar environmental conditions) should be excluded from subsequent modeling.

403 A combination of biotic and topo-climatic variables contributes to the niche of *I. webberi*.
404 Throughout modeling iterations, perennial herbaceous cover and Topographic Position Index
405 consistently contributed the most to *I. webberi* distribution, while cumulative actual
406 evapotranspiration (AET), Cosine aspect, and summer seasonal precipitation also contributed

407 to the species niche in model iterations. The perennial herbaceous cover may have constrained
408 *I. webberi* niche to areas of suitable vegetative community, thus representing a biotic
409 component of the species niche. Vegetative land cover is reported in literature as an important
410 predictor of habitat suitability for rare plants (Gogol-Prokurat 2011, McCune 2016).
411 Topographic Position Index illustrates topographic heterogeneity which impacts microclimatic
412 conditions and influences plant distribution and diversity in high-altitude and heterogeneous
413 landscapes (Chardon et al. 2014, Thornhill et al. 2017). The greater probability of *I. webberi*
414 occurrence in areas with higher cosine aspect in the 2018 and 2019 model iterations shows that
415 the species prefers cooler north-facing slopes which receive less sunlight. Though topographic
416 variables are not proximal (Austin 2002), they have been used successfully as spatial
417 delineators, and to represent missing climatic variables especially in high-altitude areas, map
418 species habitat suitability, reduce niche model overprediction, and increase model
419 performance (Lassueur et al. 2006, Fois et al. 2018).

420 Summer seasonal precipitation and AET, the bioclimatic variables, represent the
421 availability of water and energy which governs the timing of spring regeneration and seed
422 germination in *I. webberi*. Summer seasonal precipitation may play an important role in *I.*
423 *webberi* seed dispersal, as has been observed for spring-germinating plants in other cold
424 deserts of the world (Chen et al. 2019). Field observations show that *I. webberi* seeds are
425 dispersed by gravity-assisted surface run-off due to summer precipitation, resulting in the
426 colonization of interspace microsites and decolonized roads and trails. This localized seed
427 movement due to summer precipitation was also reported for *I. tweedyi* and *I. lycopodioides* var.
428 *scandularis* (Moseley 1993, Pollak 1997). Taken together, the SDM predictions are congruent

429 with field observations that *I. webberi* suitable habitats are found on gentle slopes and ridges
430 dominated by native perennial forbs, herbs, annual grasses, and fewer stands of native shrubs,
431 interspersed with bare ground or gravel-covered microsites. Unfortunately, these sites are
432 vulnerable to anthropogenic disturbances and colonization by invasive species which have
433 altered wildfire regimes in the Great Basin Desert (Chambers et al. 2014, Morris & Rowe 2014).

434 Species with small population size and restricted geographical distributions are more
435 vulnerable to future environmental changes and are frequently targets of conservation priority
436 (Lomba et al. 2010, Sousa-Silva et al. 2014). In this study, we explored the efficacy of two
437 complementary approaches for addressing the challenges associated with SDMs for rare
438 species: iterative ensemble modeling and model-guided field sampling. These two
439 complementary approaches can reduce spatial bias, allow for model fine tuning that can
440 improve model performance, and increase the chances of detecting novel locations that can
441 either fill the realized niche space or expand the species niche breadth and hence the known
442 geographical distribution. Improved model performance will enhance reliable assessment of
443 species-environment relationships. Iterative SDMs are particularly important for guiding
444 future efforts to improve species distribution datasets and allow for a tighter integration of
445 models with data, leading ultimately to more accurate and ecologically meaningful SDMs.

446

447 **ACKNOWLEDGEMENTS:** This research was funded through a grant from the U.S. Fish and
448 Wildlife Service CFDA program (award number F15AC00784), with additional funding
449 support from the Northern California Botanists (NCB) Botany research scholarship program,
450 and the Society for Conservation Biology (SCB) graduate student research fellowship. The

451 authors are grateful to the Nevada Natural Heritage Program for supplying the species
452 occurrence data and absence points for modeling. Additional data from Sarah Kulpa of the
453 U.S. Fish and Wildlife Service, Reno Field Office, Valda Lockie of the Bureau of Land
454 Management, Susanville CA Office, and the California Native Plant Society is also appreciated.
455 This work also benefited from expert advice from Dr. Town Peterson, Dr. Olivier
456 Broennimann, August (Tianxiao) Hao, and Damien Georges.

457 **REFERENCES**

- 458 Aiello-Lammens ME, Boria RA, Radosavljevic A, Vilela B, Anderson RP (2015) spThin: an R package for spatial
459 thinning of species occurrence records for use in ecological niche models. *Ecography* 38: 541-545.
460 <https://doi.org/10.1111/ecog.01132>
- 461 Allouche O, Tsoar A, Kadmon R (2006) Assessing the accuracy of species distribution models: Prevalence, kappa
462 and the true skill statistic (TSS). *J Appl Ecol* 43: 1223-1232. [https://doi.org/10.1111/j.1365-
463 2664.2006.01214.x](https://doi.org/10.1111/j.1365-2664.2006.01214.x)
- 464 Aranda SC, Lobo JM (2011) How well does presence-only-based species distribution modelling predict
465 assemblage diversity? A case study of the Tenerife flora. *Ecography* 34: 31-38.
466 <https://doi.org/10.1111/j.1600-0587.2010.06134.x>
- 467 Araújo MB, New M (2007) Ensemble forecasting of species distributions. *Trends Ecol Evol* 22: 42-47.
468 <https://doi.org/10.1016/j.tree.2006.09.010> Araújo MB, Pearson RG (2005) Equilibrium of species'
469 distributions with climate. *Ecography* 28: 693-695. <https://doi.org/10.1111/j.2005.0906-7590.04253.x>
- 470 Araújo MB, Peterson AT (2012) Uses and misuses of bioclimatic envelope modeling. *Ecology* 93: 1527-1539.
471 <https://doi.org/10.1890/11-1930.1>
- 472 Araújo MB, Rozenfeld A (2014) The geographic scaling of biotic interactions. *Ecography* 37: 406-415.
473 <https://doi.org/10.1111/j.1600-0587.2013.00643.x>
- 474 Araújo MB, Pearson RG, Thuiller W, Erhard M (2005) Validation of species-climate impact models under climate
475 change. *Global Change Biol* 11: 1054-1513. <https://doi.org/10.1111/j.1365-2486.2005.01000.x>
- 476 Banerjee AK, Mukherjee A, Guo W, Ng WL, Huang Y (2019) Combining ecological niche modeling with genetic
477 lineage information to predict potential distribution of *Mikania micrantha* Kunth in South and Southeast
478 Asia under predicted climate change. *Glob Ecol Conserv* 20: e00800.
479 <https://doi.org/10.1016/j.gecco.2019.e00800>
- 480 Beygelzimer A, Kakadet S, Langford J, Arya S, Mount D, Li S (2019) FNN: Fast Nearest Neighbor Search
481 Algorithms and Applications. R package version 1.1.3. <https://CRAN.R-project.org/package=FNN>
- 482 Borokini IT, Klingler KB, Peacock MM (2021) Life in the desert: The impact of geographic and environmental
483 gradients on genetic diversity and population structure of *Ivesia webberi*. *Ecol Evol* 11: 17537-17556.
484 <https://doi.org/10.1002/ece3.8389>
- 485 Boyce MS, Vernier PR, Nielsen SE, Schmiegelow FKA (2002) Evaluating resource selection functions. *Ecol Modell*
486 157(2-3): 281-300. [https://doi.org/10.1016/S0304-3800\(02\)00200-4](https://doi.org/10.1016/S0304-3800(02)00200-4)
- 487 Broennimann O, Fitzpatrick MC, Pearman PB, Petitpierre B, Pellissier L, Yoccoz NG, Thuiller W, Fortin M-J,
488 Randin C, Zimmermann NE, Graham CH, Guisan A. (2012) Measuring ecological niche overlap from
489 occurrence and spatial environmental data. *Glob Ecol Biogeog* 21: 481- 497.
490 <https://doi.org/10.1371/journal.pone.0049508>
- 491 Broennimann O, Thuiller W, Hughes G, Midgley GF, Alkemade JMR, Guisan A (2006) Do geographic
492 distribution, niche property and life form explain plants' vulnerability to global change? *Glob Change*
493 *Biol* 12: 1079-1093. <https://doi.org/10.1111/j.1365-2486.2006.01157.x>
- 494 Brown JL, Carnaval AC (2019) A tale of two niches: methods, concepts, and evolution. *Front Biogeog* 11: e44158.
495 <https://doi.org/10.21425/F5FBG44158>
- 496 Burns PA, Clemann N, White M (2020) Testing the utility of species distribution modelling using Random Forests
497 for a species in decline. *Austral Ecol* 45: 706-716. <https://doi.org/10.1111/aec.12884>
- 498 Chambers JC, Bradley BA, Brown CS, D'Antonio C, Germino MJ, Grace JB, Hardegree SP, Miller RF, Pyke DA
499 (2014) Resilience to stress and disturbance, and resistance to *Bromus tectorum* L. invasion in cold desert

500 shrublands of western North America. *Ecosystems* 17: 360–375. [https://doi.org/10.1007/s10021-013-](https://doi.org/10.1007/s10021-013-9725-5)
501 [9725-5](https://doi.org/10.1007/s10021-013-9725-5)

502 Chardon NI, Cornwell WK, Flint LE, Flint AL, Ackerly DD (2014) Topographic, latitudinal and climatic
503 distribution of *Pinus coulteri*: geographic range limits are not at the edge of the climate envelope.
504 *Ecography* 37: 1–12. <https://doi.org/10.1111/ecog.00780>

505 Chen Y, Shi X, Zhang L, Baskin JM, Baskin CC, Liu H, Zhang D (2019) Effects of increased precipitation on the life
506 history of spring- and autumn-germinated plants of the cold desert annual *Erodium oxyrhynchum*
507 (Geraniaceae). *AoB PLANTS* 11: plz004. <https://doi.org/10.1093/aobpla/plz004>

508 Coddington JA, Agnarsson I, Miller JA, Kuntner M, Hormiga G (2009). Undersampling bias: the null hypothesis
509 for singleton species in tropical arthropod surveys. *J. Animal Ecol.* 78: 573–584.
510 <https://doi.org/10.1111/j.1365-2656.2009.01525.x>

511 Collins SL, Glenn SM, Roberts DW (1993) The hierarchical continuum concept. *J Veg Sci* 4(2): 149–156.
512 <https://doi.org/10.2307/3236099>

513 Daly C, Halbleib M, Smith JI, Gibson WP, Doggett MK, Taylor GH, Curtis J, Pasteris PA (2008) Physiographically-
514 sensitive mapping of temperature and precipitation across the conterminous United States. *Int J Climat*
515 28: 2031–2064. <https://doi.org/10.1002/joc.1688>

516 de Siqueira MF, Durigan G, de Marco Jr. P, Peterson AT (2009) Something from nothing: Using landscape
517 similarity and ecological niche modeling to find rare plant species. *J Nat Conserv* 17: 25–32.
518 <https://doi.org/10.1016/j.jnc.2008.11.001>

519 Dilts TE, Weisberg PJ, Dencker CM, Chambers JC (2015) Functionally relevant climate variables for arid lands: a
520 climatic water deficit approach for modelling desert shrub distributions. *J Biogeog* 42: 1986–1997.
521 <https://doi.org/10.1111/jbi.12561>

522 Draper D, Marques I, Iriondo JM (2019) Species distribution models with field validation, a key approach for
523 successful selection of receptor sites in conservation translocations. *Glob Ecol Conserv* 19: e00653.
524 <https://doi.org/10.1016/j.gecco.2019.e00653>

525 Edwards Jr. TC, Cutler DR, Zimmermann NE, Geiser L, Alegria J (2004) Model-based stratifications for enhancing
526 the detection of rare ecological events. *Ecology* 86: 1081–1090. <https://doi.org/10.1890/04-0608>

527 Elith J, Leathwick JR (2009) Species Distribution Models: ecological explanation and prediction across space and
528 time. *Ann Rev Ecol Evol Syst* 40: 677–697. <https://doi.org/10.1146/annurev.ecolsys.110308.120159>

529 Elith J, Ferrier S, Huettmann F, Leathwick JR (2005) The evaluation strip: A new and robust method for plotting
530 predicted responses from species distribution models. *Ecol Modell* 186: 280–289.
531 <https://doi.org/10.1016/j.ecolmodel.2004.12.007>

532 Fois M, Cuena-Lombraña A, Fenu G, Bacchetta G (2018) Using species distribution models at local scale to guide
533 the search of poorly known species: Review, methodological issues and future directions. *Ecol Modell*
534 385: 124–132. <https://doi.org/10.1016/j.ecolmodel.2018.07.018>

535 Gogol-Prokurat M (2011). Predicting habitat suitability for rare plants at local spatial scales using a species
536 distribution model. *Ecol App* 21: 33–47. <https://doi.org/10.1890/09-1190.1>

537 Gorban A, Pokidysheva L, Smirnova E, Tyukina T (2011) Law of the minimum paradoxes. *Bull Math Biol* 73:
538 2013–2044. [10.1007/s11538-010-9597-1](https://doi.org/10.1007/s11538-010-9597-1)

539 Grant A-G, Kalisz S (2019) Do selfing species have greater niche breadth? Support from ecological niche
540 modeling. *Evolution* 74: 73–88. <https://doi.org/10.1111/evo.13870>

- 541 Guisan A, Broennimann O, Engler R, Vust M, Yoccoz NG, Lehmann A, Zimmermann NE (2006) Using niche-
542 based models to improve the sampling of rare species. *Conserv Biol* 20: 501-511.
543 <https://doi.org/10.1111/j.1523-1739.2006.00354.x>
- 544 Guisan A, Petitpierre B, Broennimann O, Daehler C, Kueffer C (2014) Unifying niche shift studies: Insights from
545 biological invasions. *Trends Ecol Evol* 29: 260–269. <https://doi.org/10.1016/j.tree.2014.02.009>
- 546 Hanley JA, McNeil BJ (1982) The meaning and use of the area under a receiver operating characteristic (ROC)
547 curve. *Radiology* 143: 29–36. <https://doi.org/10.1148/radiology.143.1.7063747>
- 548 Hanski I (1982) Dynamics of regional distribution: the core and satellite species hypothesis. *Oikos* 38: 210-221.
549 <https://doi.org/10.2307/3544021>
- 550 Harrell FE, Lee KL, Mark DB (1996) Tutorial in biostatistics multivariable prognostic models: issues in developing
551 models, evaluating assumptions and adequacy, and measuring and reducing errors. *Stat Med* 15: 361–
552 387. [https://doi.org/10.1002/\(SICI\)1097-0258\(19960229\)15:4<361::AID-SIM168>3.0.CO;2-4](https://doi.org/10.1002/(SICI)1097-0258(19960229)15:4<361::AID-SIM168>3.0.CO;2-4)
- 553 Hernandez PA, Graham CH, Master LL, Albert DL (2006) The effect of sample size and species characteristics on
554 performance of different species distribution modeling methods. *Ecography* 29: 773-785.
555 <https://doi.org/10.1111/j.0906-7590.2006.04700.x>
- 556 Hijmans RJ, Phillips S, Leathwick J, Elith J (2017) Dismo: Species Distribution Modeling. R Package Version 1.0-12.
557 <http://CRAN.R-project.org/package=dismo>
- 558 Hirzel A, Guisan A (2002) Which is the optimal sampling strategy for habitat suitability modelling. *Ecol Modell*
559 157(2-3): 331-341. [https://doi.org/10.1016/S0304-3800\(02\)00203-X](https://doi.org/10.1016/S0304-3800(02)00203-X)
- 560 Hortal J (2008) Uncertainty and the measurement of terrestrial biodiversity gradients. *J Biogeog* 35: 1335–1336.
561 <https://doi.org/10.1111/j.1365-2699.2008.01955.x>
- 562 Hutchinson GE (1957) Concluding remarks. *Cold Spring Harb Symp Quant Biol* 22: 415–427.
- 563 Ikeda DH, Max TL, Allan GJ, Lau MK, Shuster SM, Whitham TG (2016) Genetically informed ecological niche
564 models improve climate change predictions. *Glob Change Biol* 23: 164-176.
565 <https://doi.org/10.1111/gcb.13470>
- 566 Jarnevich CS, Stohlgren TJ, Kumar S, Morisette JT, Holcombe TR (2015) Caveats for correlative species
567 distribution modeling. *Ecol Inform* 29: 6-15. <https://doi.org/10.1016/j.ecoinf.2015.06.007>
- 568 Jiménez-Valverde A, Peterson AT, Soberón J, Overton JM, Aragón P, Lobo JM (2011) Use of niche models in
569 invasive species risk assessments. *Biol Invasions* 13: 2785-2797. <https://doi.org/10.1007/s10530-011-9963-4>
- 570 [4](https://doi.org/10.1007/s10530-011-9963-4)
- 571 Keinath DA, Griscom HR, Andersen MD (2014) Habitat and distribution of the Wyoming pocket gopher
572 (*Thomomys clusius*). *J Mammal* 95: 803–813. <https://doi.org/10.1644/13-MAMM-A-226>
- 573 Kraft NJ, Baldwin BG, Ackerly DD (2010) Range size, taxon age and hotspots of neoendemism in the California
574 flora. *Divers Distrib* 16: 403–413. <https://doi.org/10.1111/j.1472-4642.2010.00640.x>
- 575 Kuhn M (2008) Building Predictive models in R using the *caret* package. *J Stat Softw* 28(5): 1-26.
576 10.18637/jss.v028.i05
- 577 Kursu MB, Rudnicki WR (2010) Feature selection with the *Boruta* package. *J Stat Softw* 36(11): 1-13.
578 10.18637/jss.v036.i11
- 579 Lassueur T, Joost S, Randin CF (2006) Very high-resolution digital elevation models: Do they improve models of
580 plant species distribution? *Ecol Modell* 198(1–2): 139-153.
581 <https://doi.org/10.1016/j.ecolmodel.2006.04.004>

582 Lauzeral C, Grenouillet G, Brosse S (2012) Dealing with noisy absences to optimize species distribution models:
583 An iterative ensemble modelling approach. PLOS ONE 7: e49508.
584 <https://doi.org/10.1371/journal.pone.0049508>

585 Liu C, Wolter C, Xian W, Jeschke JM (2020) Most invasive species largely conserve their climatic niche. Proc Nat
586 Acad Sci 117: 23643-23651. <https://doi.org/10.1073/pnas.2004289117>

587 Lobo JM, Jiménez-Valverde A, Hortal J (2010) The uncertain nature of absences and their importance in species
588 distribution modelling. Ecography 33: 103–114. <https://doi.org/10.1111/j.1600-0587.2009.06039.x>

589 Lomba A, Pellissier L, Randin C, Vicente J, Moreira F, Honrado J, Guisan A (2010) Overcoming the rare species
590 modelling paradox: A novel hierarchical framework applied to an Iberian endemic plant. Biol Conserv
591 143: 2647-2657. <https://doi.org/10.1016/j.biocon.2010.07.007>

592 Marmion M, Parviainen M, Luoto M, Heikkinen RK, Thuiller W (2009) Evaluation of consensus methods in
593 predictive species distribution modelling. Divers Distrib 15: 59-69. <https://doi.org/10.1111/j.1472-4642.2008.00491.x>

594

595 McCune JL (2016) Species distribution models predict rare species occurrences despite significant effects of
596 landscape context. J Appl Ecol 53: 1871-1879. <https://doi.org/10.1111/1365-2664.12702>

597 Morris LR, Rowe RJ (2014) Historical land use and altered habitats in the Great Basin. J Mammal 95: 1144–1156.
598 <https://doi.org/10.1644/13-MAMM-S-169>

599 Moseley RK (1993) Floristic inventory of subalpine parks in the Coeur d'Alene river drainage, northern Idaho.
600 Report to Cooperative Challenge Cost-share Project Idaho Panhandle National Forests and Idaho
601 Department of Fish and Game; 62 pp.

602 Peterson AT, Papeş M, Eaton M (2007) Transferability and model evaluation in ecological niche modeling: A
603 comparison of GARP and Maxent. Ecography 30: 550–560. <https://doi.org/10.1111/j.0906-7590.2007.05102.x>

604

605 Petitpierre B, Kueffer C, Broennimann O, Randin C, Daehler C, Guisan A (2012) Climatic niche shifts are rare
606 among terrestrial plant invaders. Science 335: 1344–1348. 10.1126/science.1215933

607 Phillips SJ, Anderson RP, Schapire RE (2006) Maximum entropy modeling of species geographic distributions.
608 Ecol Modell 190: 231–259. <https://doi.org/10.1016/j.ecolmodel.2005.03.026>

609 Pili AN, Tingley R, Sy EY, Diesmos MLL, Diesmos AC (2020) Niche shifts and environmental non-equilibrium
610 undermine the usefulness of ecological niche models for invasion risk assessments. Sci Rep 10: 7972.
611 <https://doi.org/10.1038/s41598-020-64568-2>

612 Platts PJ, Ahrends A, Gereau RE, McClean CJ, Lovett JC, Marshall AR, Pellikka PKE, Mulligan M, Fanning E,
613 Marchant R (2010) Can distribution models help refine inventory-based estimates of conservation
614 priority? A case study in the Eastern Arc forests of Tanzania and Kenya. Divers Distrib 16: 628-642.
615 <https://doi.org/10.1111/j.1472-4642.2010.00668.x>

616 Pollak O (1997) Morphology and dynamics of alpine populations of *Ivesia lycopodioides* ssp. *scandularis* from the
617 White Mountains of California. Univ Cal White Mount Res Station Symp 1: 97– 116.

618 R Core Team (2020) R: A language and environment for statistical computing. R Foundation for Statistical
619 Computing, Vienna, Austria. [online]. Available from URL: <http://www.R-project.org/>

620 Ramesh V, Gopalakrishna T, Barve S, Melnick DJ (2017) IUCN greatly underestimates threat levels of endemic
621 birds in the Western Ghats. Biol Conserv 210: 205– 221. <https://doi.org/10.1016/j.biocon.2017.03.019>

622 Regos A, Gagne L, Alcaraz-Segura D, Honrado JP, Domínguez J (2019) Effects of species traits and environmental
623 predictors on performance and transferability of ecological niche models. Sci Rep 9: 4221.
624 <https://doi.org/10.1038/s41598-019-40766-5>

- 625 Rinnhofer LJ, Roura-Pascual N, Arthofer W, Dejaco T, Thaler-Knoflach B, Wachter GA, Christian E, Steiner FM,
626 Schlick-Steiner BC (2012) Iterative species distribution modelling and ground validation in endemism
627 research: An Alpine jumping bristletail example. *Biodiv Conserv* 21: 2845–2863.
628 <https://doi.org/10.1007/s10531-012-0341-z>
- 629 Särkinen T, Gonzáles P, Knapp S (2013) Distribution models and species discovery: the story of a new *Solanum*
630 species from the Peruvian Andes. *PhytoKeys* 31: 1–20. <https://doi.org/10.3897/phytokeys.31.6312>
- 631 Singh NJ, Yoccoz NG, Bhatnagar YV, Fox JL (2009) Using habitat suitability models to sample rare species in
632 high-altitude ecosystems: a case study with Tibetan argali. *Biodiv Conserv* 18: 2893–2908.
633 <https://doi.org/10.1007/s10531-009-9615-5>
- 634 Sofaer HR, Jarnevich CS, Pearse IS, Smyth RL, Auer S, Cook GL, Edwards Jr. TC, Guala GF, Howard TG,
635 Morisette JT, Hamilton H (2019) Development and delivery of species distribution models to inform
636 decision-making. *BioScience* 69: 544–557. <https://doi.org/10.1093/biosci/biz045>
- 637 Sousa-Silva R, Alves P, Honrado J, Lomba A (2014) Improving the assessment and reporting on rare and
638 endangered species through species distribution models. *Global Ecol Conserv* 2: 226–237.
639 <http://dx.doi.org/10.1016/j.gecco.2014.09.011>
- 640 Stockwell DRB, Peterson AT (2002) Effects of sample size on accuracy of species distribution models. *Ecol Modell*
641 148: 1–13. [https://doi.org/10.1016/S0304-3800\(01\)00388-X](https://doi.org/10.1016/S0304-3800(01)00388-X)
- 642 Strubbe D, Broennimann O, Chiron F, Matthysen E (2013) Niche conservatism in non-native birds in Europe:
643 niche unfilling rather than niche expansion. *Global Ecol Biogeog* 22: 962–970.
644 <https://doi.org/10.1111/geb.12050>
- 645 Svejcar T, Boyd C, Davies K, Hamerlynck E, Svejcar L (2017) Challenges and limitations to native species
646 restoration in the Great Basin, USA. *Plant Ecol* 218: 81–94. <https://doi.org/10.1007/s11258-016-0648-z>
- 647 Thornhill AH, Baldwin BG, Freyman WA, Nosratinia S, Kling MM, Morueta-Holme N, Madsen TP, Ackerly DD,
648 Mishler BD (2017) Spatial phylogenetics of the native California flora. *BMC Biol* 15: 96.
649 <https://doi.org/10.1186/s12915-017-0435-x>
- 650 Thuiller W, Lafourcade B, Engler R, Araújo MB (2009) BIOMOD – a platform for ensemble forecasting of species
651 distributions. *Ecography* 32: 1–5. <https://doi.org/10.1111/j.1600-0587.2008.05742.x>
- 652 Töpel M, Antonelli A, Yesson C, Eriksen B (2012) Past climate change and plant evolution in Western North
653 America: a case study in Rosaceae. *PLOS ONE* 7: e50358. <https://doi.org/10.1371/journal.pone.0050358>
- 654 U.S. Fish and Wildlife Service [USFWS] (2014) Species Report for *Ivesia webberi* (Webber’s ivesia). Nevada Fish
655 and Wildlife Office, Reno. United States Fish and Wildlife Service. Accessed at
656 [https://www.fws.gov/nevada/nv_species/documents/webber_ivesia/ivwe_species_report1_8_14_fina](https://www.fws.gov/nevada/nv_species/documents/webber_ivesia/ivwe_species_report1_8_14_final.pdf)
657 [l.pdf](https://www.fws.gov/nevada/nv_species/documents/webber_ivesia/ivwe_species_report1_8_14_final.pdf)
- 658 U.S. Geological Survey [USGS] (2017) 1 Arc-second Digital Elevation Models (DEMs) – USGS National Map 3DEP
659 Downloadable Data Collection. U.S. Geological Survey. Accessed at [https://www.usgs.gov/core-](https://www.usgs.gov/core-science-systems/ngp/tnm-delivery/)
660 [science-systems/ngp/tnm-delivery/](https://www.usgs.gov/core-science-systems/ngp/tnm-delivery/)
- 661 Valavi R, Elith J, Lahoz-Monfort JJ, Guillera-Aroita G (2019) blockCV: An R package for generating spatially or
662 environmentally separated folds for k-fold cross-validation of species distribution models. *Meth Ecol*
663 *Evol* 10: 225–232. <https://doi.org/10.1111/2041-210X.13107>
- 664 Vaughan IP, Ormerod SJ (2003) Improving the quality of distribution models for conservation by addressing
665 shortcomings in the field collection of training data. *Conserv Biol* 17: 1601–1611.
666 <https://doi.org/10.1111/j.1523-1739.2003.00359.x>
- 667 Warren DL, Seifert SN (2011) Ecological niche modeling in Maxent: The importance of model complexity and the
668 performance of model selection criteria. *Ecol Appl* 21(2): 335– 342. <https://doi.org/10.1890/10-1171.1>

- 669 Warren DL, Glor RE, Turelli M (2008) Environmental niche equivalency versus conservatism: quantitative
670 approaches to niche evolution. *Evolution*, 62(11), 2868-2883. [https://doi.org/10.1111/j.1558-
671 5646.2008.00482.x](https://doi.org/10.1111/j.1558-5646.2008.00482.x)
- 672 Weiss A (2001) Topographic position and landform analysis. Poster presentation, ESRI User Conference, San
673 Diego, California, USA.
- 674 Whittaker RJ, Araújo MB, Paul J, Ladle RJ, Watson JEM, Willis KJ (2005) Conservation biogeography: assessment
675 and prospect. *Divers Distrib* 11: 3-23. <https://doi.org/10.1111/j.1366-9516.2005.00143.x>
- 676 Williams JN, Seo C, Thorne J, Nelson JK, Erwin S, O'Brien J, Schwartz MW (2009) Using species distribution
677 models to predict new occurrences for rare plants. *Divers Distrib* 15: 565-576.
678 <https://doi.org/10.1111/j.1472-4642.2009.00567.x>
- 679 Wisz MS, Hijmans RJ, Li J, Peterson AT, Graham CH, Guisan A, NCEAS Predicting Species Distributions
680 Working Group (2008) Effects of sample size on the performance of species distribution models. *Divers
681 Distrib* 14: 763-773. <https://doi.org/10.1111/j.1472-4642.2008.00482.x>
- 682 Witham CW (2000) Current Knowledge and Conservation Status of *Ivesia webberi* A. Gray (Rosaceae), the Webber
683 ivesia, in Nevada. Status Report prepared for the Nevada Natural Heritage Program, Dept. of
684 Conservation and Natural Resources, Carson City, NV. 52pp.
- 685 Xian G, Homer C, Meyer D, Granneman B (2013) An approach for characterizing the distribution of shrubland
686 ecosystem components as continuous fields as part of NLCD. *ISPRS J Photogramm Remote Sens* 86: 136-
687 149. <https://doi.org/10.1016/j.isprsjprs.2013.09.009>
- 688

689 **TABLES**690 **Table 1. Iterative niche modeling with increasing number of presence and absence points**691 **for *Ivesia webberi*.**

Year	Presence points	Raw absence points	Thinned absence	Predictor variables used for final modeling
2015	23	758	53	Perennial herbaceous cover, Topographic Position Index (TPI) and annual evapotranspiration
2018	26	1652	90	Perennial herbaceous cover, TPI and cosine aspect
2019	27	1881	75	Perennial herbaceous cover, TPI and cosine aspect
2020	32	2289	102	Perennial herbaceous cover, TPI and summer mean precipitation

692

693 **Table 2. Descriptions of six uncorrelated predictor variables used to fit preliminary niche**
 694 **models for *Ivesia webberi*. The three predictor variables used for the iterative niche models**
 695 **were selected from this pool. All predictors were resampled to 30 m resolution**

Predictor variable	Relationship with species
Actual evapotranspiration (AET)	An estimate of the amount of water removed from an area by both evaporation and transpiration. AET, a direct predictor, is a proxy estimate of plant productivity
Cosine aspect	Higher values indicate north-facing slopes, which receive less sunlight
Perennial herbaceous vegetative cover	A spatial vegetative cover delineation representing native grasses, perennial forbs, and cacti, which includes areas of <i>I. webberi</i> distribution. It is considered a representation of biotic interactions and accounting for community assemblage in sites harboring <i>I. webberi</i>
Minimum monthly temperature	A direct predictor that potentially influences plant distribution (Araújo & Rozenfeld, 2014). Vegetative and seed regeneration of <i>I. webberi</i> are dependent on cold stratification that characterizes late winter and early spring seasons
Summer seasonal precipitation	A direct predictor that potentially influences plant distribution. Summer precipitation causes surface runoffs which facilitate localized gravity-enhanced seed dispersal and colonization of empty niches. Precipitation and temperature in winter and spring seasons influence the phenology of <i>I. webberi</i>
Topographic position index (TPI)	A scale-dependent variable describing the elevation of a cell in relation to the mean elevation of the neighboring cells. At the scale of 333 m, TPI distinguishes between mountains and valleys in the study area. The study area is characterized by topographic heterogeneity which can limit dispersal and distribution, and also act as proxy for microclimatic conditions

696

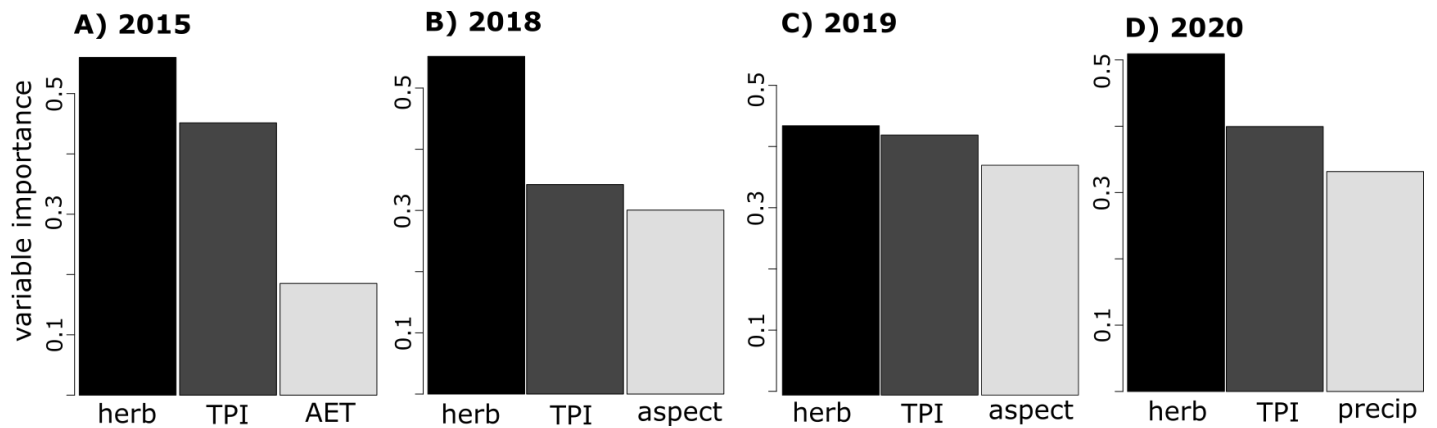
697 **Table 3. Niche density, predicted habitat suitability, and distance of new locations to the nearest neighbor in the**
 698 **initial points**

Location name	Finding	Year	Niche density	Predicted habitat suitability	Distance from known location (km)
Wildcat Hill	Opportunistic: discovered by Bureau of Land Management (BLM) staff during land surveys	2018	0.27	0.73	8.07
Unit 6 extension	Model: predicted suitable sites near known location	2018	0.87	0.59	0.38
Smoke Creek Road	Opportunistic: discovered during California Native Plant Society vegetative surveys	2019	0.86	0.37	62.98
Unit 4 extension	Model: high predicted suitability	2020	0.38	0.62	0.03
South end of HJWA	Model: high predicted suitability	2020	0.58	0.64	2.99
HJWA south end #2	Model: suitable sites near known location	2020	0.71	0.30	2.26
Private land discovery #1	Model: suitable sites near known location	2020	0.21	0.21	1.39
Private land discovery #2	Model: suitable sites near known location	2020	0.36	0.28	2.23
New Smoke Creek Road	Model: suitable sites near known location	2020	0.83	0.15	1.22

700 FIGURES

701

702



703

704

705

706

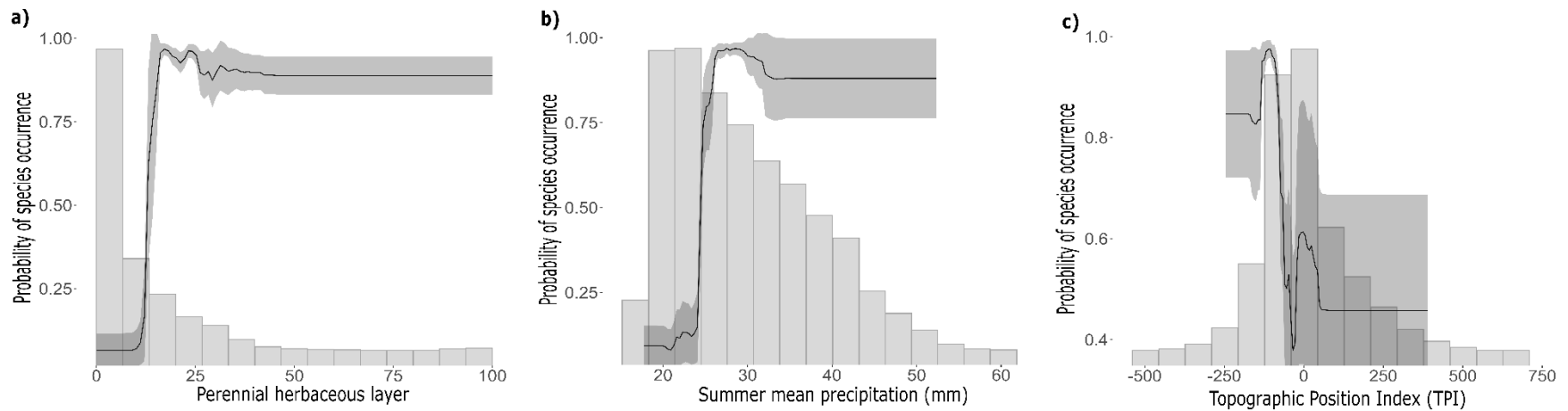
707

708

709

Figure 1. Variable contributions to the iterative niche modeling for *Ivesia webberi* from (a) 2015 to (d) 2020. The three predictors used for each year of iterative modeling were selected from the preliminary modeling. Herb represents the perennial herbaceous vegetative cover, TPI stands for Topographic Position Index at 333 m, AET stands for cumulative actual evapotranspiration, aspect represents cosine-transformed aspect, while precip stands for summer mean precipitation

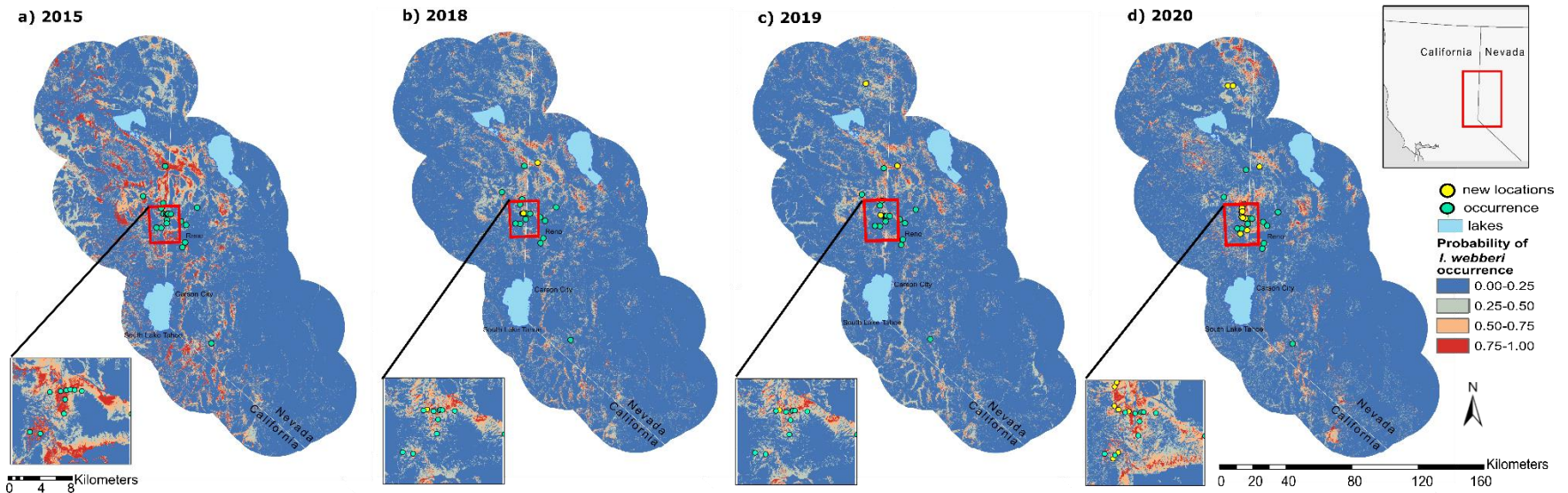
710



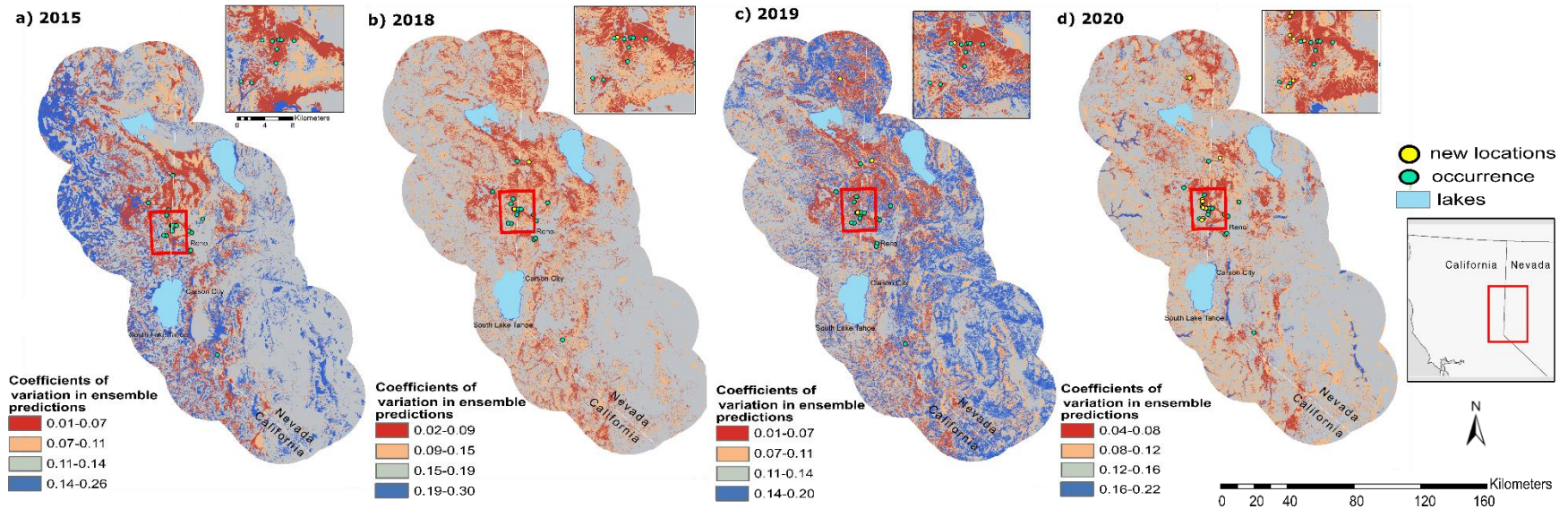
711

712 **Figure 2.** Partial response plots showing the predicted probability of *Ivesia webberi* occurrence in a) Perennial herbaceous
713 vegetative cover, b) summer mean precipitation, and c) Topographic Position Index. The partial response plots were
714 generated using the Boosted Regression Trees, while the histogram represent the predicted values from 10,000 randomly
715 sampled background points from the three variables used for the niche modeling. The partial response plots for each of
716 the 10 model replicates of the six SDM algorithms is included in Figure S1 Supplemental Information.

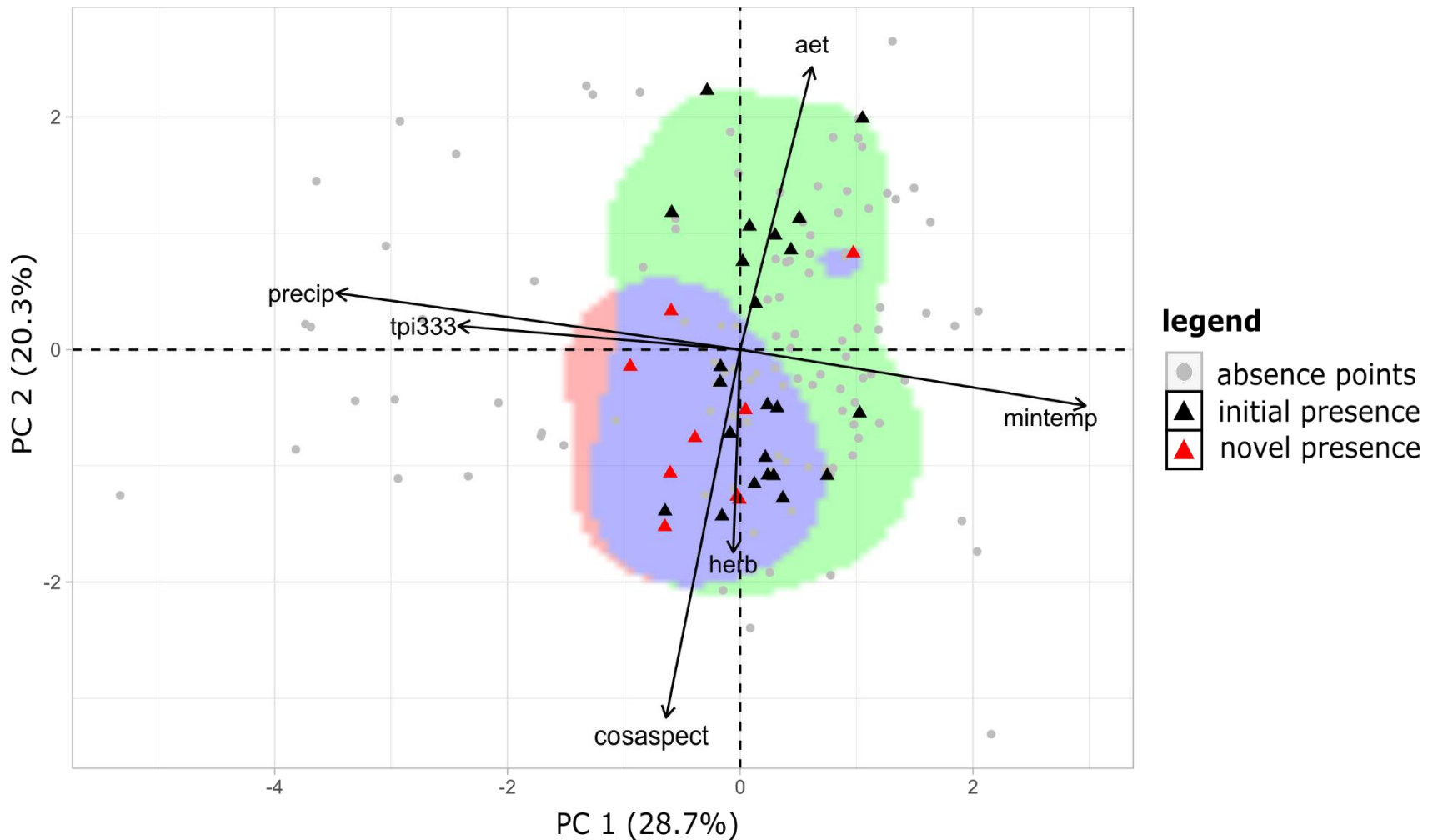
717



718
 719 **Figure 3.** Maps of the predicted geographical distribution of *Ivesia webberi* in the western Great Basin Desert, with both the
 720 original and new occurrence points overlay. Red colored pixels represent areas of predicted high probability of *I. webberi*
 721 occurrence, orange pixels represent intermediate probability of species occurrence, while blue pixels are predicted areas
 722 of zero to low probability of occurrence. The occurrence points in green are the original *I. webberi* occurrence points used
 723 for niche modeling, while yellow colored occurrence points represent the novel populations



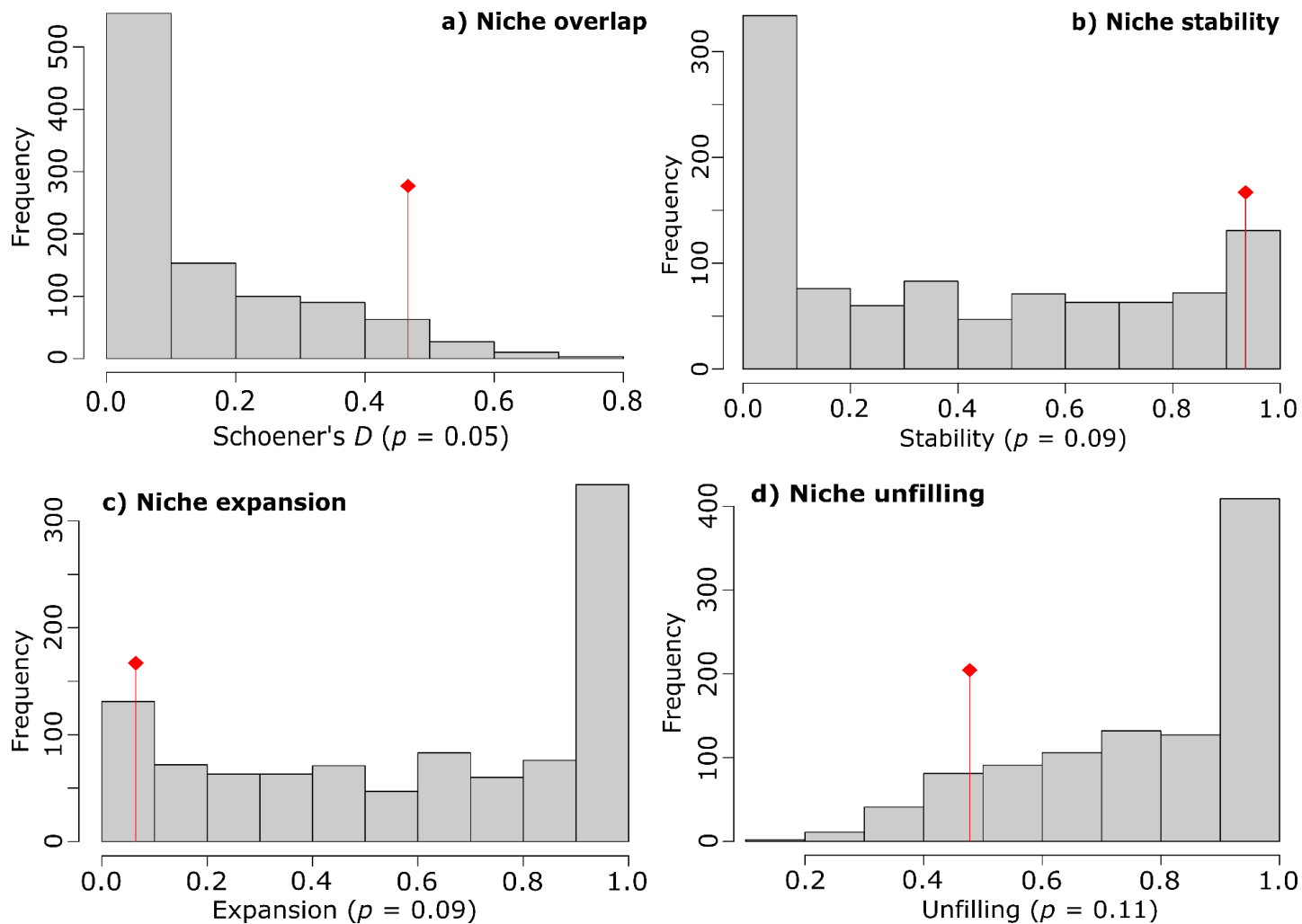
725
726 **Figure 4.** Maps of the coefficients of variation within the ensemble predictions of *Ivesia webberi* in the western Great Basin
727 Desert, with both the original and new occurrence points overlay. Red colored pixels represent areas of low prediction
728 uncertainty, orange pixels represent intermediate prediction uncertainty, while blue pixels are predicted areas of high
729 uncertainty in model predictions.



730

731 **Figure 5.** PCA biplot of the environmental predictors that influence *Ivesia webberi* niche in the western Great Basin Desert.
 732 These absence and presence data are combinations of initial (black) and new locations (red). The green area on the plot
 733 represents the environmental niche occupied only by the initial occurrences (unfilling), while the blue area represents a
 734 subset of the initial niche occupied by both initial and novel occurrences (stability) and pink colored areas represent a
 735 portion of the niche occupied only by the new locations (expansion).

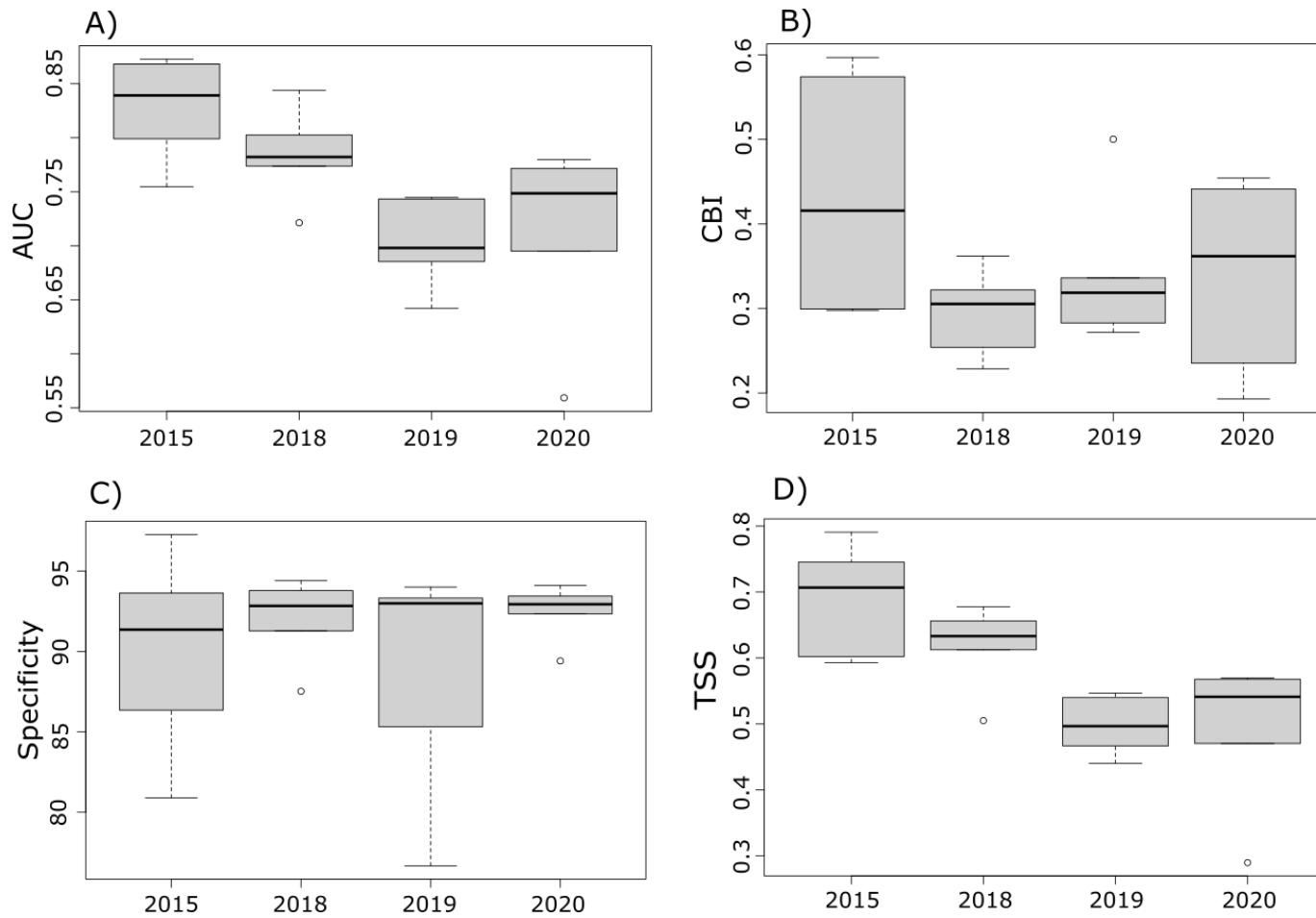
736



737

738 **Figure 6.** Histogram plots of the randomized values for (a) niche overlap, measured as the Schoener's D , (b) niche
 739 stability, (c) niche expansion, and (d) niche unfilling between the initial and novel occurrence locations for *Ivesia webberi*.
 740 The red bar on each plot represents the actual niche metric. For each niche estimate, 1000 randomizations were done
 741 using a niche similarity test that randomly shifts the centroids of the initial and novel realized niches.

742



743

744 **Figure 7.** Boxplots of the mean values (n=10 replicates each for six algorithms) of model performance in (a) area under
 745 curve (AUC) of the receiver operating characteristic (ROC) plot, (b) Boyce index (BI), (c) specificity, and (d) true skill
 746 statistic (TSS) across the years of iterative niche modeling (shown in x axes).

747